



POLISH-JAPANESE ACADEMY
OF INFORMATION TECHNOLOGY

Department of Computer Science
Specialization of Intelligent Data Processing Systems

Łukasz Piotrak
s18002

An analysis of dimensionality reduction and
music information retrieval techniques for the
visual representation of large audio datasets.

Bachelor of Science
Thesis Supervisor: Sinh Hoa Nguyen

Warsaw, Poland, February 2021

Abstract

Navigation and search has long been a bottleneck activity when working with sound. Recent advancements in dimensionality reduction techniques have made it possible to replace the classic directory tree with a spacial map of audio files, resulting in a more intuitive representation. I provide a method of evaluating visualizations using methods from spatial statistics and find that a combination of PCA + STFT + UMAP methods gives the best scoring, although unexpected 2D embedding on a dataset of instrument recordings.

Przeszukiwanie zbiorów plików od dawna sprawia trudność w efektywnej pracy z dźwiękiem. Wraz z postępem w dziedzinie redukcji wymiarowości danych, powstała możliwość zastąpienia klasycznej przeglądarki plików na bardziej intuicyjną reprezentację, tj. przestrzenną mapę plików audio. W tej pracy przedstawiam metodę na ocenę wygenerowanych przestrzennych reprezentacji poprzez zastosowanie metod ze statystyki przestrzennej. Przeprowadzam także analizę porównawczą metod ekstrakcji cech oraz redukcji wymiarowości i odkrywam, że połączenie metod PCA + STFT + UMAP daje najlepszą, mimo nieregularnych reprezentacji dla zbioru danych składających się z krótkich nagrań gry na instrumentach.

Contents

1	Introduction	4
1.1	Related Work	5
1.1.1	The infinite drum machine	5
1.1.2	Klustr	5
2	Background	7
2.1	Music Information Retrieval	7
2.1.1	Short-time Fourier Transform (STFT)	7
2.1.2	Mel Frequency Cepstral Coefficients (MFCC)	9
2.1.3	MIR metrics	11
2.2	Dimensionality reduction	13
2.2.1	Principal Component Analysis (PCA)	13
2.2.2	t-Distributed Stochastic Neighbour Embedding (t-SNE) .	14
2.2.3	Uniform Manifold Approximation and Projection (UMAP)	17
2.3	Evaluation metrics	19
2.3.1	Silhouette Score	20
2.3.2	Roundness	20
2.3.3	Overlap of cluster convex hulls	21
2.3.4	Ripley's K function	21
3	Experiment design and overview	22
3.1	Dataset	22
3.2	The processing pipeline	22
3.3	Preprocessing	24
3.4	Feature Extraction	24
3.4.1	Short-time Fourier Transform (STFT)	25
3.4.2	MFCC	25
3.4.3	Music Information Retrieval Metrics	25
3.5	Feature Manipulation	26
3.6	Dimensionality Reduction	28
3.7	Scoring the plots	30

4 Experiment Evaluation	33
4.1 Overall Results	33
4.2 The Ripley metric	36
4.3 The Silhouette Measure	36
4.4 Future work	37
4.5 Conclusion	43
Bibliography	44
Appendices	47
A Source Code	47

Introduction

The current paradigm for the storage and organization of audio files is that of the classic directory tree. This results in an attribute ontology; files are grouped together into classes (usually by directory name) i.e. “Drums”, “Vocals” and assigned a range of attributes by means of file name or tags. This approach is limited, e.g. the file might be labeled incorrectly or the labels might not adequately describe the sound. Moreover, many properties inherent to the files are hard to represent e.g. two audio samples might be in separate branches of the taxonomy but be perceptually similar. However, as shown by projects such as The Infinite Drum Machine by Google Creative Lab [9], collections of sounds can be explored more naturally with the help of dimensionality reduction techniques.

drums	Acetone Rhythm Ace	28	MaxV - XE8 Block 1 ext_14.wav
field_r~	Acetone Rhythm King	10	MaxV - XE8 Block 2 ext_15.wav
instrum~	Acetone Rhythm Master	7	MaxV - XE8 Clap int_15.wav
loops	AJK Percusyn	10	MaxV - XE8 Cowbell 1 ext_12.wav
sounds~	Akai MPC-2000	9	MaxV - XE8 Cowbell 2 ext_13.wav
vocals	Akai MPC60	18	MaxV - XE8 Crash ext_11.wav
AKAI XE-8		31	MaxV - XE8 Crash int_13.wav
	Akai XR-1	10	MaxV - XE8 ElectroTom int_4.wav
	Akai XR10	62	MaxV - XE8 Hat Closed ext_4.wav
	Alesis D4fx	54	MaxV - XE8 Hat Closed int_5.wav
	Alesis DM5	470	MaxV - XE8 Hat Medium int_6.wav

Figure 1.1: Browsing sound samples using a directory structure.

Advances in this area have enabled the intuitive representation of high-dimensional data. The dimension count of a Dataset can be reduced arbitrarily while still preserving information about its intrinsic properties. Commonly, this approach is used to plot Datapoints as clouds in 2D or 3d space, allowing for a depiction of the data which can be naturally grasped by the human mind.

As with many kinds of information, audio data in its raw form is unfit for such processing. An intermediate representation must be constructed if any insights are to be gleaned from the data. In order to obtain a representations of audio signals useful to a human observer, a selection of features

have to be extracted, which might correspond to certain aspects of the human perception of sound. These can then be used as inputs to produce a visualization by means of dimensionality reduction.

1.1 Related Work

There have been a number of papers and software projects with a focus on dimensionality reduction as applied to audio datasets. This work is based on previous efforts in this domain, such as those by Hantrakul & Sarwate [16] and McDonald et. al [9] which I will describe in more detail below. I expand upon their findings by using a dataset of samples containing harmonic data, widening the pool of feature extraction methods and introducing a novel method of assessing the visualizations using Ripley's H function to measure the homogeneity of density distribution of the plots.

1.1.1 The infinite drum machine

The idea for this work originally came from the excellent web app by McDonald et. al [9]. The app organized thousands of foley sounds on a 2D plane using the t-SNE technique introduced by van Der Maaten & Hinton [18]. Similar sounding samples were placed close together. Sounds could be navigated and played back by hovering over individual points with the mouse. A sequencer was implemented to enable the arrangement of those sounds into audio loops. As far as my research showed this was one of the first applications introducing the excellent idea of using dimensionality reduction techniques to make intuitive “maps” of large audio collections. Since the app was meant more as a proof of concept I immediately saw areas in which it might be extended. Firstly, it only worked on a static dataset, meaning there was no way to make visualizations for other datasets or even add new samples to the existing visualization. Secondly, the functionality was extremely limited by the intended use case. A user is able to select several sounds and use them as samples to program a musical loop and not much besides.

1.1.2 Klustr

Klustr, by Hantrakul & Sarwate [16] is a review of feature extraction methods and dimensionality reduction algorithms as applied to a large audio dataset. The authors used a dataset of 10,000 drum samples, shortened to a length of 0.25 seconds. The feature sets used were: Short-time-Fourier-Transform, Mel-Frequency Cepstral Coefficients, various Music Information Retrieval

features (RMS, Spectral Centroid, Spectral Crest, Spectral Flux, Spectral Rolloff, Zero-Crossing Rate) and finally features extracted by a Wavenet autoencoder. These features were then applied to a dimensionality reduction step using 3 different dimensionality reduction techniques: PCA, t-SNE and UMAP. The scoring function is a combination of the silhouette coefficient [1], roundness of plots measured by the Polsby-Popper test [14] and the ratio of overlap of convex hulls of the different drum classes. I have used a similar scoring system, though changing the calculation of the ratio of overlap of convex hulls and adding another scoring method. The authors determined that, for the dataset used, a combination of STFT, PCA and UMAP yielded the best 2D visualization.

Background

2.1 Music Information Retrieval

With the recent rise of music streaming platforms, which serve millions of users each day, extracting information from music to classify, categorize and build effective recommender systems seems more relevant than ever. The objective of Music information retrieval (MIR) is the extraction of such information. It is a broad field of study, which lies on the intersection of many different research domains. It uses knowledge from musicology and music theory, (music) psychology, psycho-acoustics, audio engineering, computer science and machine learning. It is rapidly growing in scope, with a rapid increase in published papers in the last few years.

MIR may be subdivided into two distinct subdomains. The first focused mainly on the analysis of non-audio music formats such as musical notation, song lyrics and even user reviews and bibliographical information (publication date, title etc). And the second, Audio Content Analysis (ACA), which uses various techniques from digital signal processing, machine learning, statistics and psychoacoustics, among others, to extract meaningful information from audio signals. Many techniques from ACA are used in machine learning, notably speech recognition and other fields, to extract psycho-acoustic features from raw pulse-code modulated signals.

There are a wide range of features which describe different statistical, physical and perceptual aspects of sound. Some of the most commonly used in the field of MIR are described below.

2.1.1 Short-time Fourier Transform (STFT)

The Short-time Fourier Transform is a representation of a signal obtained by taking the Fourier transform of short segments of time. The method used to obtain the STFT is relatively straightforward. First, the signal is divided

into shorter, equal-length segments using a window function. These segments usually have some overlap in order to prevent artifacts of the original signal (so-called spectral leakage) Multiple window functions could be used for this step, however a Hann window is usually used. Usually a window length of 10 to 300ms is chosen. Smith [17] points out three reasons for doing so:

- The human ear analyzes short fragments of signals at a time (10-20ms).
- Signals change over time. It is best to analyze over a time frame where the spectral content stays relatively constant.
- Computation of the fourier transform is costly and computing a whole signal at once may inefficient and undesirable.

Next, the Discrete Fourier Transform (DFT) is computed for each segment:

$$S_i(k) = \sum_{n=1}^N s_i(n)h(n)e^{-j2\pi kn/N} \quad 1 \leq k \leq K \quad (2.1)$$

Where $s_i(n)$ is the i-th window of the original signal, $h(n)$ is an analysis window of N samples and K is the length of the DFT. We can thus observe how the frequency content of the signal changes as we progress through time.

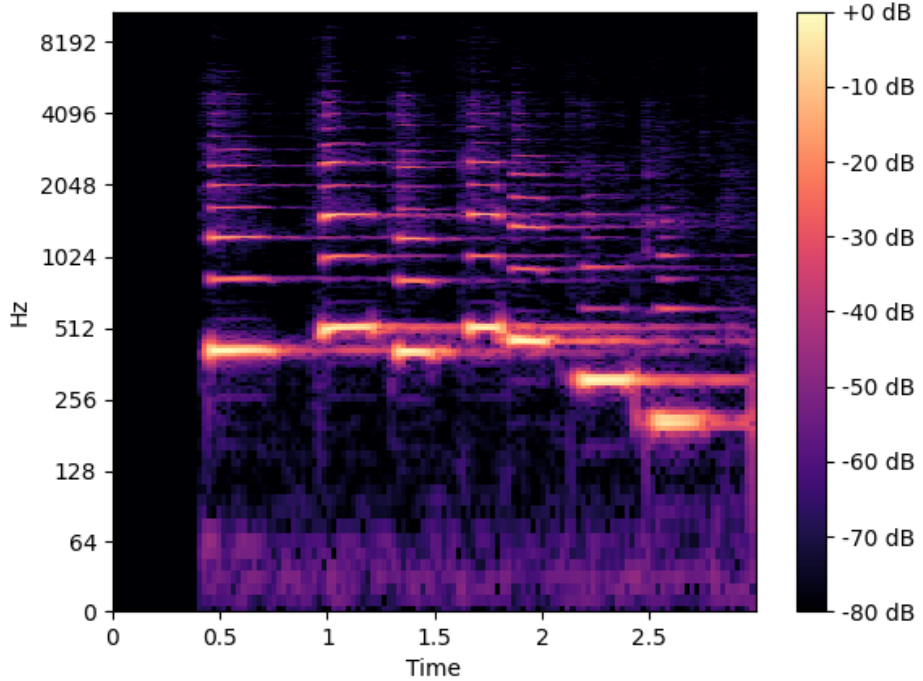


Figure 2.1: An STFT spectrogram

2.1.2 Mel Frequency Cepstral Coefficients (MFCC)

Davis and Mermelstein [4] first introduced the concept of MFCC in 1980. Several parametric representations of acoustic signals were compared with an emphasis placed on providing a way of distinguishing between phonetically similar monosyllabic words. This resulted in the development of a compact representation, which could provide an efficient way of reflecting phonetic differences between phonemes. Inspired by the observation that humans perceive sound in a logarithmic, not linear scale. A key component to the success of the MFCC representation is the initial transformation of the signal using the Mel-filterbank seen in 2.3. Earlier work by Pols [13], suggested that a cosine series expansion on these Mel-filtered frequency energies which might yield an efficient representation of audio signals for speech recognition systems. An example MFCC spectrogram can be seen in 3.4. The main steps for calculating MFCC may be summarized as follows:

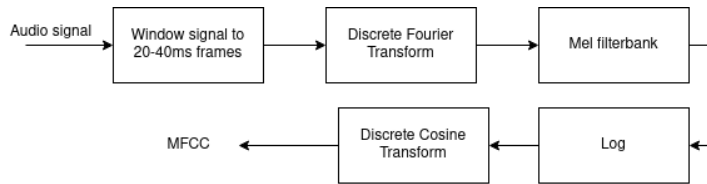


Figure 2.2: A high-level diagram of the MFCC calculation algorithm.

1. Split the signal into windowed fragments using a window function, typically a Hamming window is used [3] with a period of 20-40ms. This period allows us to obtain a reliable estimate of the spectral features at the particular window while also roughly corresponding to the temporal resolution of human hearing. A longer period would mean losing information about the spectral variation.
2. Similarly to the calculation of STFT, the Discrete Fourier Transform 2.1 is applied to each window:

$$|Y(k)|^2 = \left| \sum_{n=1}^M y(n) \cdot e^{(-j2\pi nk)} \right|^2$$

where $1 \leq k \leq M$. Usually, a 512 frequency bin DFT is calculated but only the first 257 are used in later steps.

3. Next, the Mel filterbank is applied to each window (shown in 2.3) to convert the frequencies to the Mel scale. The Mel scale is used because the human perception of sound is more sensitive to differences in pitch

at low rather than high frequencies. The formula for converting from the frequency scale to the Mel scale is:

$$M(f) = 2595 \log_{10}(1 + f/700)$$

Commonly, 26 filters are used and applied to the result of the previous step. To calculate the filterbank energies, each filterbank (the length of which corresponds to the length of the periodogram) is multiplied with the power spectrum. The result is summed, the result of which indicates the amount of energy in the periodogram power spectrum for that particular filterbank. The result of this step is 26 coefficients corresponding to the 26 filterbank energies. The output filterbank energies may be calculated as:

$$e(i) = \sum_{k=1}^M |Y(k)|^2 \cdot \psi_i(k)$$

4. The log for each filterbank energy is taken.
5. The Discrete Cosine Transform (DCT) is taken for each filterbank energy log, giving 26 cepstral coefficients. In effect this gives the formula:

$$MFCC_m = \sqrt{\frac{2}{Q}} \sum_{l=0}^{Q-1} \log[e(l+1)] \cdot \cos \left[m \cdot \left(\frac{2l-1}{2} \right) \cdot \frac{\pi}{Q} \right]$$

Where $0 \leq m \leq R - 1$, R is the number of cepstrum coefficients.

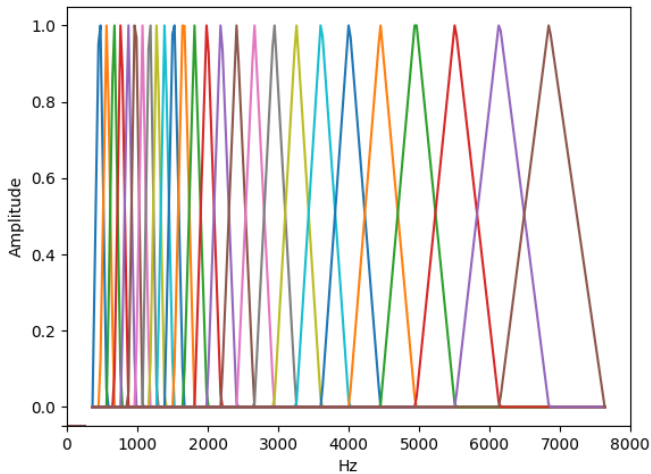


Figure 2.3: The mel filterbank

2.1.3 MIR metrics

Spectral Centroid

The mean of the normalized distribution over frequency per frame of a spectrogram.

$$\text{centroid}(t) = \frac{\sum_{k=b_1}^{b_2} f_k s_k}{\sum_{k=b_1}^{b_2} s_k}$$

where:

- f_k is the frequency value at bin k .
- b_1 and b_2 are the bin boundaries between which to calculate the centroid.
- s_k is the amplitude at k

Spectral Rolloff

The frequency for each window such that at least k percent of the energy of the spectrum is contained in this frequency bin and the bins below. The rolloff point is i such that:

$$\sum_{k=b_1}^i s_k = k \sum_{k=b_1}^{b_2} s_k$$

where:

- s_k is the amplitude at bin k .
- b_1 and b_2 are the bin boundaries between which to calculate the spread.
- k is the percentage of energy contained between b_1 and i .

Spectral Bandwidth

Given by:

$$(\sum_k s_k (f_k - f_c)^p)^{\frac{1}{p}}$$

where:

- $s(k)$ is the amplitude at bin k .
- $f(k)$ is the bin at k .
- f_c is the spectral centroid at k .

Spectral Crest

The crest of the power spectrum over time. Given by:

$$\text{crest} = \frac{\max(s_k \in [b_1, b_2])}{\frac{1}{b_2 - b_1} \sum_{k=b_1}^{b_2} s_k}$$

where:

- s_k is the amplitude at bin k .
- b_1 and b_2 are the bin boundaries between which to calculate the crest.

Spectral Flux

Can intuitively be thought of as how much the signal changes over time. Given by:

$$\text{flux}(t) = \left(\sum_{k=b_1}^{b_2} |s_k(t) - s_k(t-1)|^p \right)^{\frac{1}{p}}$$

where:

- s_k is the amplitude at bin k .
- b_1 and b_2 are the bin boundaries between which to calculate the flux.
- p is the normalization type.

Spectral Flatness

Measures how much noise-like a sound is. Given by:

$$\text{flatness} = \frac{\left(\prod_{k=b_1}^{b_2} s_k \right)^{\frac{1}{b_2 - b_1}}}{\frac{1}{b_2 - b_1} \sum_{k=b_1}^{b_2} s_k}$$

where:

- s_k is the amplitude at bin k .
- b_1 and b_2 are the bin boundaries between which to calculate the flux.

Root-Mean-Square (RMS)

The root-mean-square. Given by:

$$\text{RMS} = \sqrt{\frac{1}{N} \sum_{n=1}^N |x_n|^2}$$

Zero-Crossing Rate

How many times a signal crosses zero a given time frame.

2.2 Dimensionality reduction

2.2.1 Principal Component Analysis (PCA)

PCA is an orthogonal linear transformation, which projects data onto a new system of axes. The projection is such that the first axis accounts for the greatest variance in the data, the second axes for the second greatest, and so on. The computation is described as follows:

1. Normalization.

By transforming each variable to be in the same scale.

$$\text{Norm}(x) = \frac{x - \mu(X)}{\sigma(X)}$$

2. Computing the covariance matrix

If we have a vector of random variables (X_1, \dots, X_n) then the covariance matrix is defined as:

$$K_{XX} = \begin{bmatrix} \text{Cov}(X_1, X_1) & \dots & \text{Cov}(X_1, X_n) \\ \vdots & \ddots & \vdots \\ \text{Cov}(X_n, X_1) & \dots & \text{Cov}(X_n, X_n) \end{bmatrix}$$

Where $\text{Cov}(X_i, Y_i)$ is defined as:

$$\text{Cov}(X_i, Y_i) = E(X_i X_j) - E(X_i)E(X_j)$$

$E(X_i)$ is the expected value given as:

$$E(X_i) = \sum_{j=1}^k x_j p_j$$

and p_j is the probability of x_j .

Since $\text{Cov}(X_i, X_j) = \text{Var}(X_j)$, the diagonal is composed of the variances of each variable. Also, since covariance is commutative ($\text{Cov}(X_i, X_j) = \text{Cov}(X_j, X_i)$), the matrix is symmetric with respect to the diagonal.

3. Calculate the Principal Components of the covariance matrix

Principal Components (or eigenvectors) for a linear transformation are the vectors which stay on their own span (the line running through the vectors beginning and end). Knowing this property we can define it as an equation for a transformation A , eigenvector v and eigenvalue λ :

$$Av = \lambda v \quad (2.2)$$

After inserting an identity matrix (I) and bringing all to the left side:

$$Av - \lambda Iv = 0$$

Since v must be non-zero we can use the determinant. From this equation we should get a polynomial. The roots of this polynomial give us the eigenvalues.

$$\det(A - \lambda I) = 0$$

Once the eigenvalues are known we can easily determine the corresponding eigenvector by solving for v in 2.2.

Now, the eigenvectors can be ordered by their eigenvalues. We can compute the percentage of variance accounted for by each component by dividing the eigenvalue of a component by the sum of eigenvalues.

4. Project the standardized data onto axes represented by the Principal Components

$$P = C^T D^T$$

Where P is the projected data, C the matrix containing the Principal Components and D the original, standardized data.

2.2.2 t-Distributed Stochastic Neighbour Embedding (t-SNE)

t-Distributed Stochastic Neighbour Embedding is a nonlinear dimensionality reduction technique used for embedding high-dimensional datasets into 2 or 3 dimensions. It is based on the original Stochastic Neighbour Embedding (SNE), developed by Roweis and Hinton [8] in 2002 and improved by Maaten and Hinton [18] in 2008 by adding the use of the t-distribution. The steps for calculating t-SNE may be described as follows:

1. Begin by converting of the Euclidean distances between points in the original dataset into conditional probabilities that represent how similar points are to each other. From the original t-SNE paper: “The similarity of datapoint x_j to datapoint x_i is the conditional probability, $p_{j|i}$, that x_i would pick x_j as its neighbor if neighbours were picked in proportion to their probability density under a Gaussian centered at x_i .” In essence, this means that points which are close together in the original dataset are have a high value $p_{j|i}$ while those which are further away obtain lower values in proportion to their distance. The condition $p_{j|i}$ is given by:

$$p_{j|i} = \frac{\exp\left(\frac{-||x_i - x_j||^2}{2\sigma_i^2}\right)}{\sum_{k \neq i} \exp\left(\frac{-||x_i - x_k||^2}{2\sigma_i^2}\right)}$$

Where σ_i is the variance of the Gaussian that is centered on datapoint x_i . There is most likely no single σ_i optimal for all datapoints as the density of the data will often vary depending upon the point in question. A particular value of the variance gives a probability distribution P_i over all the other datapoints. A binary search is performed to find the value of σ_i , that produces a P_i with a perplexity value, which is given as a parameter to the t-SNE algorithm, defined as:

$$Perp(P_i) = 2^{H(P_i)}$$

where $H(P_i)$ is the entropy of P_i :

$$H(P_i) = -\sum_j p_{j|i} \log p_{j|i}$$

The probability is defined as:

$$p_{ij} = \frac{p_{j|i} + p_{i|j}}{2N}$$

with $p_{ij} = p_{ji}$, $p_{ii} = 0$ and $\sum_{i,j} p_{ij} = 1$.

2. Next, a measure of similarity is defined between two points (y_i and y_j) in the low dimensional embedding. If d is the number of dimensions, then $y_i \in \mathbb{R}^d$:

$$q_{ij} = \frac{\exp(1 + ||y_i - y_j||^2)^{-1}}{\sum_k \sum_{l \neq k} \exp(1 + ||y_k - y_l||^2)^{-1}}$$

As previously $q_{ii} = 0$. Here, the distribution is Student's t-distribution with one degree of freedom. The distribution is chosen because $(1 + ||y_i - y_j||^2)^{-1}$ approaches an inverse square law for large distances between points in the low-dimensional map. This allows dissimilar data-points to be modeled as far apart in the low-dimensional embedding.

The points are then distributed randomly throughout the low-dimensional space.

3. Gradient descent is performed on the low-dimensional embedding of the data in such a way as to minimize the Kullback-Leibler divergence between p and q . The divergence is defined as:

$$KL(P||Q) = \sum_i \sum_j p_{ij} \log \frac{p_{ij}}{q_{ij}}$$

The gradient descent minimizes a Kullback-Leibler divergence between a joint probability distribution P and the joint probability distribution Q :

$$C = KL(P||Q)$$

In general, the cost is large if widely separated points in the embedding are used to represent points which are nearby in the original data (using a small q_{ij} to model a large $p_{j|i}$). Conversely using nearby embedding points to represent widely separated datapoints has a small cost. This gives a focus on retaining local structure in the embedding. The final gradient descent function is:

$$\frac{\delta C}{\delta y_i} = 4 \sum_j (p_{ij} - q_{ij})(y_i - y_j)(1 + ||y_i - y_j||^2)^{-1}$$

2.2.3 Uniform Manifold Approximation and Projection (UMAP)

Similar to t-SNE, UMAP is a nonlinear technique for dimension reduction. It was developed by McInnes et. al. in 2018. Advertised as being able to preserve more global structure and having a superior run time than t-SNE, UMAP has seen a giant growth in popularity in the last few years (4.9k Github stars vs 823 of Maatens official implementation o Barnes-Hut t-SNE). Unlike t-SNE it has no restrictions on embedding dimensions, which means it can be used as a general-purpose dimensionality reduction technique for machine learning.

An overview of the UMAP algorithm is presented below:

Algorithm 1: High-level UMAP algorithm

Input: X : Set of datapoints
 n : the neighborhood size to use for local metric approximation
 d : the dimension count of the reduction
min-dist: a parameter specifying the minimum distance between points in the embedding
n-epochs: a parameter controlling how much work to perform
Output: Y : Dataset with reduced dimensions

```

for  $x \in X$  do
|  $SS \leftarrow \bigcup_{x \in X} \text{localFuzzySimplicialSet}(X, x, n)$ 
end
 $Y \leftarrow \text{spectralEmbedding}(SS, d)$ 
 $Y \leftarrow \text{optimizeEmbedding}(SS, Y, \text{min-dist}, \text{n-epochs})$ 
return  $Y$ 
```

This process starts by the construction of local fuzzy simplicial sets for each datapoint. These are constructed by finding the n nearest neighbors according to a selected distance metric. Next a normalized, approximate distance between the neighbors on the manifold is calculated as seen in algorithm 3. The next step is the construction of the union of all local fuzzy simplicial sets after which Spectral embedding is performed as shown in algorithm 4. The last step is the optimization of the embedding by minimizing the fuzzy set cross entropy by using stochastic gradient descent as shown in algorithm 5.

Algorithm 2: localFuzzySimplicialSet

Input: X : Set of datapoints
 x : Datapoint to calculate the local simplicial set for
 n : the neighborhood size to used for local metric approximation
Output: fs-set: output fuzzy simplicial set

```

knn, knn-dists  $\leftarrow$  approxNN( $X, x, n$ )
 $\rho \leftarrow$  knn-dists[1]
 $\sigma \leftarrow$  smoothKNNDist(knn-dists,  $n, \rho$ )
fs-set0  $\leftarrow X$  Fuzzy set image of 0-simplices
fs-set1  $\leftarrow \{([x, y], 0) | y \in X\}$  Fuzzy set image of 1-simplices
for  $y \in knn$  do
     $d_{x,y} \leftarrow \max(0, \text{dist}(x, y) - \rho) / \sigma$ 
    fs-set1  $\leftarrow$  fs-set1  $\cup ([x, y], \exp(-d_{x,y}))$ 
end
return fs-set

```

Algorithm 3: smoothKNNDist

Input: knn-dists: distances of k-nearest neighbors
 n : the neighborhood size to used for local metric approximation
 ρ : Distance to nearest neighbor
Output: σ : normalizing factor for distances

```

binSearch(knn-dists) such that
 $\sum_{i=1}^n \exp(-(knn\text{-dists}_i - \rho) / \sigma) = \log_2(n)$  return  $\sigma$ 

```

Algorithm 4: spectralEmbedding

Input: top-rep: Fuzzy simplicial set representation of the data

d : the neighborhood size to used for local metric approximation

Output: Y : Spectral embedding

```

 $A \leftarrow$  1-skeleton of top-rep expressed as a weighted adjacency matrix
 $D \leftarrow$  degree matrix for the graph  $A$ 
 $L \leftarrow D^{1/2}(D - A)D^{1/2}$ 
evec  $\leftarrow$  sorted Eigenvectors of  $L$ 
 $Y \leftarrow$  evec[1 ...  $d + 1$ ]
return  $Y$ 
```

Algorithm 5: Optimizing the embedding

Input: top-rep: Fuzzy simplicial set representation of the data

Y : Spectral embedding

$min-dist$: The minimum distance between points in the embedding

$n-epochs$: number of iterations used for optimization

Output: Y : optimized embedding

```

 $\alpha \leftarrow 1.0$ 
Fit  $\phi$  from  $\psi$  defined by min-dist
for  $e \leftarrow 1, \dots, n-epochs$  do
  for  $([a, b], p) \in top-rep_1$  do
    if  $Random() \leq p$  then
       $y_a \leftarrow y_a + \alpha * \delta(\log(\phi))(y_a, y_b)$ 
      for  $i \leftarrow 1, \dots, n-neg-samples$  do
         $c \leftarrow random\ sample\ from\ Y$ 
         $y_a \leftarrow y_a + \alpha * \delta(\log(\phi))(y_a, y_c)$ 
      end
    end
  end
   $\alpha \leftarrow 1.0 - e/n-epochs$ 
end
return  $Y$ 
```

2.3 Evaluation metrics

After reducing the dimensionality of the dataset to 2 dimensions, a scatter plot may be constructed with each audio file being represented as a single point. Below are detailed description of measures I chose to describe the

correctness and usability of plots.

2.3.1 Silhouette Score

The Silhouette Score is a measure of how well an algorithm clusters data. More precisely, it measures how closely a datapoint resembles other points from its own cluster compared with other clusters. The score is generally higher for convex, well-separated and dense clusters.

$$s(i) = \frac{a(i) - b(i)}{\max\{a(i), b(i)\}}$$

Where $a(i)$ is the mean distance between a sample $i \in C_k$ and all other points in the same cluster C_k . This gives us how close a point is to the corresponding cluster. It is given by the equation:

$$a(i) = \frac{1}{|C_k| - 1} \sum_{j \in C_k, i \neq j} d(i, j)$$

where $d(i, j)$ is the distance between points i and j .

b is the mean distance between a sample $i \in C_k$ and all other points in the nearest cluster C_l . Given by:

$$b(i) = \min_{l \neq k} \frac{1}{|C_l|} \sum_{j \in C_l} d(i, j)$$

The final Silhouette score for a clustering is the mean Silhouette Coefficient over all the datapoints:

$$\frac{1}{|I|} \sum_{i \in I} s(i)$$

Where I is the set of all datapoints. The final value is in the range $[-1, 1]$ with values closer to -1 indicating incorrect clusters and values closer to $+1$ indicating highly dense clusters. Scores around zero indicate overlapping clusters.

2.3.2 Roundness

The overall roundness of the plot is calculated by using the method proposed by Polsby & Popper [14]:

$$PP(D) = \frac{4\pi A(D)}{P(D)^2}$$

where D is the convex hull of all points on the plot, $P(D)$ is the circumference and $A(D)$ the area.

2.3.3 Overlap of cluster convex hulls

The measure of overlap of the convex hulls of each class. I calculate this by taking the ratio of the area of the union of convex hulls of each class to the sum of areas of the convex hulls of each cluster:

$$O = \frac{A(U)}{\sum_{c \in C} A(H_c)}$$

Where $A(U)$ is the union of all convex hulls, $A(H_c)$ is the area of the Hull for class c and C is the set of all classes.

2.3.4 Ripley's K function

Ripley's K function is a method used in spatial analysis to describe how a collection of points are distributed over a given area. It provides a measure of how clustered, dispersed or randomly distributed the measured phenomenon appears to be in the area of interest. The function is sum of the number of points N within a distance r of a selected point p , per area λ surrounding p . This value is normalized by the total number of points:

$$K(r) = \frac{\sum_{i=1}^n N_{p_i}(r)}{n\lambda}$$

It may be interpreted as a measure of deviation of a given distribution from the random Poisson distribution. In essence, this lets us measure the homogeneity of the spatial density of the data points. The expected value of $K(r)$ for a random distribution is πr^2 . If the output value deviates from this value, this indicates clustering or dispersion in the data. The K-function may be normalized so that the expected value is r :

$$L(r) = \sqrt{K(r)/\pi}$$

Further normalization gives an expected value of 0, called the H-function:

$$H(r) = L(r) - r$$

Now, a positive value of $H(r)$ indicates that the data is clustered at the scale of r . If the value is negative, the data is dispersed.

Experiment design and overview

3.1 Dataset

I used the Medley-Solos-db dataset assembled by Lostanlen et al. [11]. Downloaded through the *mirdata* Python library [2]. The dataset consists of 21572 mono WAV files sampled at 44.1 kHz at a bit depth of 32. Every audio clip has a duration of 2972 milliseconds. The data is split into 3 subsets: training, validation and test. Each sample belongs to one instrument category among a taxonomy of 8. Each instrument class was given a distinct color for easier recognition on the plots as seen in 3.1. I use the training subset of this dataset. The distribution of sounds is summarized in table

clarinet	elec. guitar	f. singer	flute	piano	tenor sax	trumpet	violin
732	955	1142	3167	2609	325	406	2899

Table 3.1: The distribution of instrument classes

3.2 The processing pipeline

To produce a 2D scatter plot of the dataset, the original audio files, each an array of 65,536 floating-point numbers, has to be reduced to 2 values. The process can be thought of as having 4 distinct steps. A short overview of the pipeline is given below. Each step is then described in greater detail.

1. Preprocessing.

The audio files are ingested in a format which is easy to run calculations on. In this case a numpy ndarray.

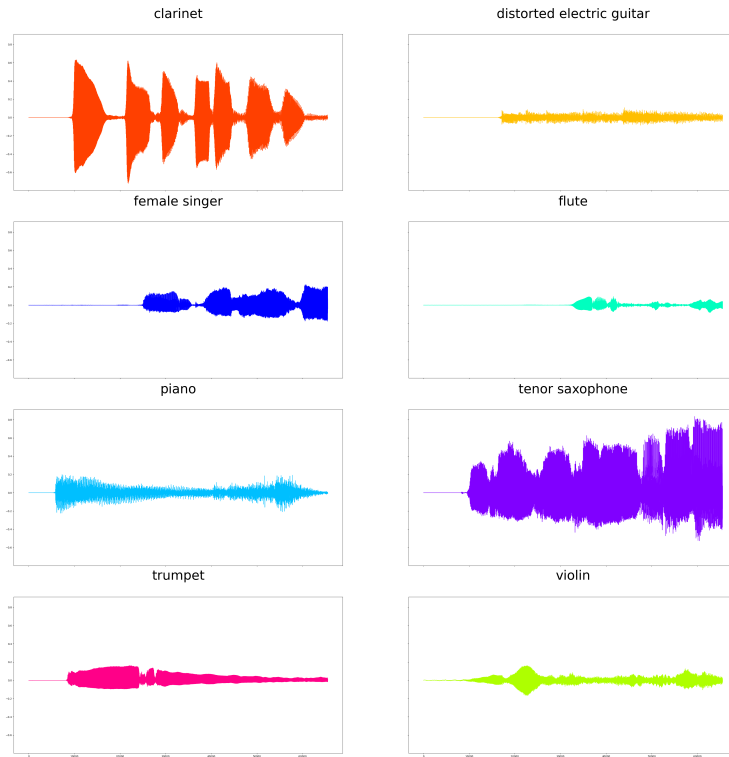


Figure 3.1: Selected sample belonging to each of the instrument classes. Each consists of 65,536 32-bit floating point numbers.

2. Feature Extraction.

Characteristics of the sound are extracted using a selection of algorithms and mathematical tools found in 3.2. These are then used as an intermediate representation of the sound for further processing.

3. Feature manipulation

Some of the features had to be further modified after extraction. The operations include reshaping feature matrices and aggregation.

4. Dimensionality Reduction.

After selecting a set of features to serve as a representation of the original files PCA, t-SNE or UMAP is used to reduce them to two

dimensions.

Once the plots have been generated, the one which most closely fits the defined criteria must be chosen. As such, an extra, fourth step in which plots are evaluated is added.

3.3 Preprocessing

The data is ingested using the Librosa python library [12] used for music and audio analysis. The “librosa.load” method was used to convert the WAV files to a float32 numpy ndarray.

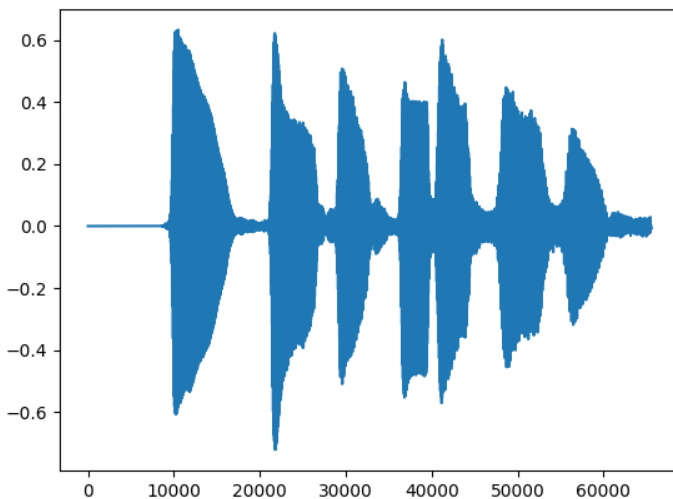


Figure 3.2: A sample from the clarinet class

After loading the samples, the amplitudes were normalized to be in the range $[-1, 1]$ by dividing by the max amplitude value for the sample. The data loaded in such a way was stored in a hdf5 file.

3.4 Feature Extraction

Finding a compact representation of phenomena is crucial for machine learning processes, including dimensionality reduction. To produce a meaningful representation of the raw data, useful to machines as well as humans, the step of extracting features is required. It can be even thought of as a preliminary dimensionality reduction technique as a raw signal consisting of many

thousands of values to just a handful, which, with luck, provide an adequate representation of useful characteristics, innate to the signal. Most of the feature extraction steps were calculated using the implementations found in the librosa library.

3.4.1 Short-time Fourier Transform (STFT)

The Short-time Fourier Transform is a basic representation in signal processing, which captures the change in frequency content over time. To extract the STFT, I used the librosa implementation. I decided to take the STFT over 32 windows in both the time and frequency domains, finally giving a 32x32 matrix:

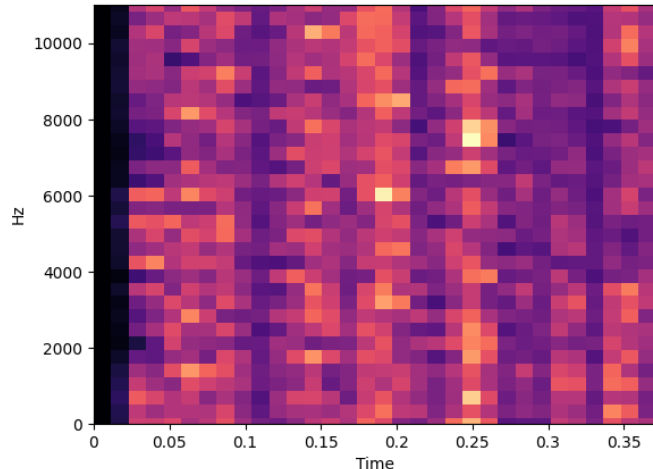


Figure 3.3: STFT of the sample in figure 3.2

3.4.2 MFCC

The Mel-Frequency Cepstral Coefficients are a heavily used in both speech recognition and Music Information Retrieval [7, 16, 15, 5]. I used the librosa implementation to calculate the MFCC's. I decided to go with 20 Cepstral Coefficient and a hop length of 256, resulting in a feature size of 20x257:

3.4.3 Music Information Retrieval Metrics

A number of metrics from the field of audio analysis has also found to be useful when extracting timbre information from audio signals [5, 16]. In my

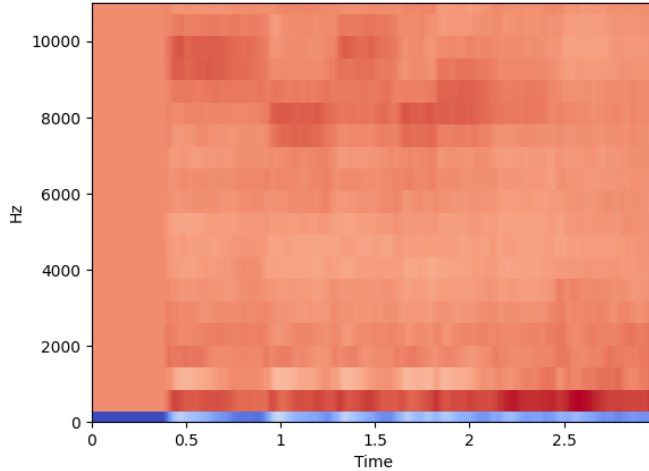


Figure 3.4: MFCC of the sample in figure 3.2

case these will include all those described in 2.1.3

3.5 Feature Manipulation

Many of the features are of different shapes and sizes. Since the matrix passed to the dimensionality reduction algorithm must be rectangular (i.e. a vector for each sample) a way must be found to force the features into a 1D vector of values. I have used two approaches.

- **Flattening**

If the feature matrix is 2 dimensional, we can simply concatenate consecutive rows into one feature vector transforming a (k, n) shape matrix to an array of length $k \times n$. The raw STFT and MFCC feature matrices must be flattened in this way to be used in the further steps of dimensionality reduction.

- **Aggregation over selected axis**

Another approach to reducing feature dimensions is that of aggregation. We can calculate an aggregate value over a particular axis, in essence reducing the dimensionality of the matrix by this axis. We can then treat the reduced matrix as any other feature vector. As suggested

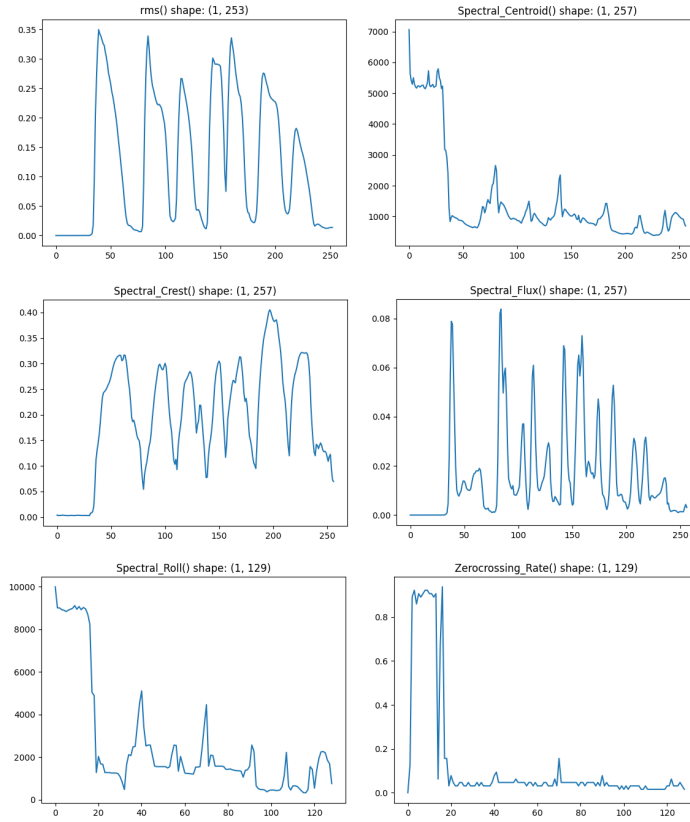


Figure 3.5: Graphs of MIR features for the sample in figure 3.2

by Dupont et al. [6] and Fedden [7], I chose three aggregation functions: the *average*, *standard deviation*, and the *mean of the difference* between consecutive values in the vector.

In my case this procedure was applied to obtain the following four features:

- Raw STFT, reducing size from 32x32 -> 32x3. I call this “statistically shortened STFT”
- Raw MFCC, reducing size from 20x257 -> 20x3. I call this “statistically shortened MFCC”
- A second time to the statistically shortened STFT, reducing size from 32x3 -> 3. I call this “vertically statistically shortened STFT”
- A second time to the statistically shortened MFCC, reducing size from 20x3 -> 3. I call this “vertically statistically shortened

MFCC”

Inspired by the successes of Klustr [16], with using a preliminary dimensionality reduction step on raw features using PCA before feeding applying dimensionality reduction proper, I also tried this approach on the raw STFT and MFCC features. I decided to make features out of the top n principal components, where n took the values: [3, 5, 8, 12, 20].

The final list of features is shown in table 3.2

Metric Name	Dimensions	Description
STFT	32x32	Original STFT
stat STFT	32x3	statistically shortened STFT
vert stat STFT	3	vertically statistically shortened STFT
PCA 3 STFT	3	First 3 principal components of the original STFT
PCA 5 STFT	3	First 5 principal components of the original STFT
PCA 8 STFT	8	First 8 principal components of the original STFT
PCA 12 STFT	12	First 12 principal components of the original STFT
PCA 20 STFT	20	First 20 principal components of the original STFT
MFCC	20x257	Original MFCC
stat MFCC	20x3	statistically shortened MFCC
vert stat MFCC	3	vertically statistically shortened MFCC
PCA 3 MFCC	3	First 3 principal components of the original MFCC
PCA 5 MFCC	3	First 5 principal components of the original MFCC
PCA 8 MFCC	8	First 8 principal components of the original MFCC
PCA 12 MFCC	12	First 12 principal components of the original MFCC
PCA 20 MFCC	20	First 20 principal components of the original MFCC
stat STFT + stat MFCC	52x3	stat MFCC appended to stat STFT
all mir	8x3	statistically shortened mir metrics
reduced mir	6x3	mir metrics without rms and centroid
PCA 3 MFCC + reduced mir	7x3	reduced mir with PCA 3 MFCC
PCA 3 STFT + reduced mir	7x3	reduced mir with PCA 3 STFT

Table 3.2: All feature sets used for the dimensionality reduction step

3.6 Dimensionality Reduction

The last step in the pipeline is the final dimension reduction of the final collection of features to just 2 values. 4 different algorithms were used in this step:

- **Principal Component Analysis**

The basic, tried-and-tested dimensionality reduction method. This method doesn't accept any additional parameters except the number of Principal Components to output. As such, for each collection of features we obtain 1 plot.

- **t-Stochastic Neighbour Embedding**

What has come to be a widespread technique in the field of machine learning for its ability to create useful 2D maps of data. Used by McDonal et al. and Hantrakul et al. to create visualizations of audio data. t-SNE's uses extend far beyond just audio data, however. It is commonly used in the field of single-cell genomics to visualize human genetic data [10] and is able to separate samples from different continents and even reflects some local, sub-continental patterns.

3 parameters influence the visualization in a significant way:

- **Perplexity**

Which can be interpreted as how much attention the algorithm should give to local or global structure. In the original article van der Maaten & Hinton suggested that perplexity values should generally fall in the range 5-50. In my case, smaller values tend to result in plots with less dense clusters with higher values giving more well-separated clusters. I chose the values [5, 10, 20, 40, 60] as parameters for the t-SNE plots.

- **Learning rate**

Usually falls in the range [10-10000]. I however determined that values higher than 1000 seemed to lose global structure. I chose the values [20, 50, 100, 200, 300]

- **Number of iterations**

I decided to go with a constant value of 3000. After heuristic tests I determined that the plots seemed to be stable for this dataset.

- **Uniform Manifold Approximation and Projection**

A relatively new dimensionality reduction method. It is very effective at preserving both the local and global structure of the original data in its projections. Similarly to t-SNE it is also based on manifold learning. The important hyperparameters are:

- **number of neighbours**

This parameter controls the number of approximate nearest neighbours to use to construct the initial high dimensional graph. Low values tend to focus on the fine, local structure. Higher values put an emphasis on the wider structure since they take into account a larger number of neighbour points. I chose values [5, 10, 15, 30, 50, 100, 200]

- **minimum distance**

is the value used by the algorithm to determine what the minimum distance points on the embedding can be from each other. I chose to sweep through the whole range: [0.0, 0.001, 0.01, 0.1, 0.5, 0.75, 0.99]

Since the objective is to make a round and homogenously dispersed plot, while still keeping the clusters separate, I suspect that values which strike a balance between being globally spread out and having enough detailed local structure to separate the clusters will be evaluated as the best.

3.7 Scoring the plots

The experiment was designed with a particular goal in mind - generating plots from the original audio data which would enable an intuitive grasp of the dataset. In order to achieve this, I define several metrics for evaluating the plots:

- How well the embedding reflects the inherent relationships between datapoints. This is measured by the Silhouette score with the class labels corresponding to cluster labels. Also, the overlap of the convex hulls of classes is an indicator of this quality.
- Readability and ease-of-navigation of the plot. In order for the plot to be readable, points should be as evenly distributed as possible, avoiding clumps, which might be hard to navigate. Ripley's function is an indicator of homogeneity of the density distribution of points on the plot. I figured, that a regular, uniform shape of the plot would increase readability, as such metric of readability is given by the Polsby-Popper method for measuring the roundness of the convex hull of the plot.

Each plot produced is scored using these metrics. Since each of these metrics had a different range of values, to compute a final score for the plot, each metric was normalized to the range [0, 1]. The final score for plot $p \in P$ is a

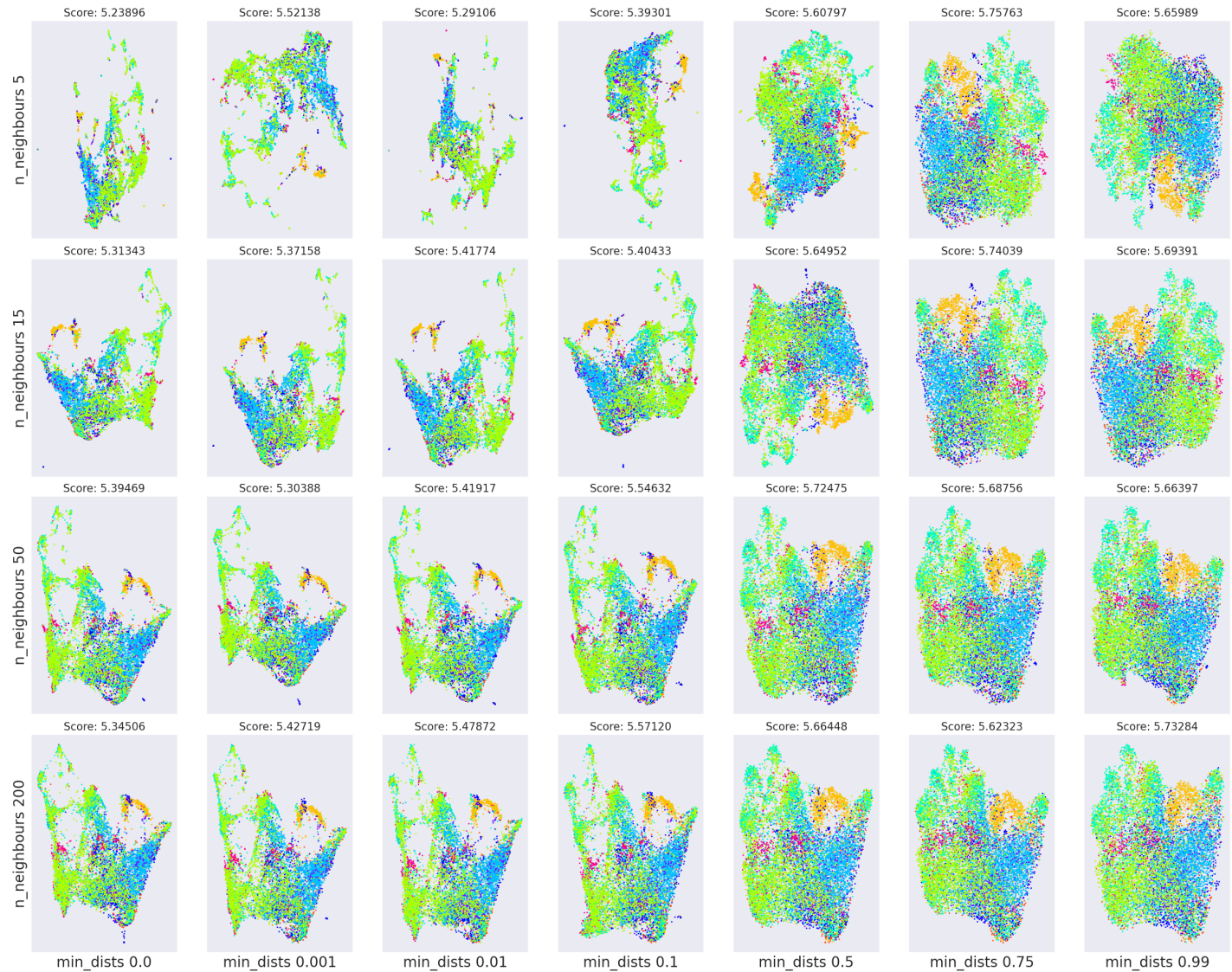


Figure 3.6: A UMAP parameter sweep with STFT as the feature. It is clear to see that lower values of hyperparameters (top left) give more densely clustered plots with a focus on the local structure, while higher values (bottom right) are more distributed and focus more on global relationships.

weighted sum of all the normalized individual metrics given by:

$$T(p) = 2\text{silhouette}(p) + 2\text{ripley}(p) + \text{overlap}(p) + \text{roundness}(p)$$

Where:

- $\text{silhouette}(p)$ is the normalized Silhouette score. Because the silhouette metric is in the range $[-1, 1]$ the value must be shifted to be in range $[0, 1]$: $s(p) + 1$. Where $s(p)$ is the Silhouette score for the plot. The shifted silhouette score is then normalized relative to the max silhouette score, finally giving:

$$\text{silhouette}(p) = \frac{s(p) + 1}{\max\{s(p)|p \in P\}}$$

- $\text{ripley}(p)$ is a metric based on the Ripley H-function. First, the average Ripley H-function is taken for plot p for radii in the set: $R = (0.05, 0.1, 0.25, 0.5) \sum_{r \in R} H_p(r)$ Since the H-function can assume values both negative and positive, I decided to take the absolute value. This causes a loss of information, since negative values indicate dispersion and positive ones indicate clustering. However, this distinction is not important for the purposes of the experiment. The only information important to us is how much the plot deviates from being uniformly dense. Since we want values close to 1 to indicate a better score I take the inverse, giving:

$$H(p) = \text{abs}\left(\frac{\sum_{r \in R} H_p(r)}{|R|}\right)^{-1}$$

With $H_p(r)$ being Ripley's H-function for plot p taken for radius r . Finally, the value is normalized relative to the max value for all plots.

$$\text{ripley}(p) = \frac{H(p)}{\max\{H(p)|p \in P\}}$$

- $\text{overlap}(p)$ is the ratio of overlap of convex hulls for the clusters to the area of the whole plot. Normalized relative to the max value for all plots:

$$\text{overlap}(p) = \frac{O(p)}{\max\{O(p)|p \in P\}}$$

- $\text{roundness}(p)$ is calculated using the Polsby-Popper method. Also normalized relative to the max value for all plots:

$$\text{roundness}(p) = \frac{PP(p)}{\max\{PP(p)|p \in P\}}$$

Experiment Evaluation

4.1 Overall Results

The final, best scoring plots for different feature sets are shown in 4.1, 4.2, 4.3. Most of the plots separate the instrument classes relatively well. They also seem to exhibit a round and fairly uniform structure. The exceptions are plots which have gone through a preliminary PCA reduction step, leaving 3 principal components. These are labeled *PCA 3 STFT* and *PCA 3 MFCC*. The interesting, string-shaped plots only appear with the combination of *PCA 3 STFT* and *PCA 3 MFCC* with *UMAP*. This is most probably a side-effect of the way in which UMAP builds its high dimensional representation of the data by using a fuzzy simplicial complex. UMAP always connects points to their nearest neighbour in the high-dimensional representation. I hypothesize that the string-like shapes are the joined nearest neighbours. UMAP then decides that the global structure contained in the 3d PCA plot shown in 4.4 is best represented by spacing the strings as visible in the plots. A closer look at the UMAP grid search (4.5) reveals that this is most probably the case. The more nearest neighbours the UMAP algorithm uses to determine connectedness in the high-dimensional representation, the more pronounced becomes the pattern.

This phenomenon is all the more interesting when we take a look at the top scoring plots overall, shown in 4.6. All the best scoring plots are from this particular feature set.

This result is counterintuitive. It seems that many of the other plots would score better on each metric. The plots seem to be less clustered and less uniformly distributed. When looking closely at the values, we can see that the silhouette and overlap scores for the *PCA 3* plots are very close to the scores of the other plots. However, when we look at the Ripley score, we see that these plots have values significantly closer to zero (meaning a higher score after normalization).

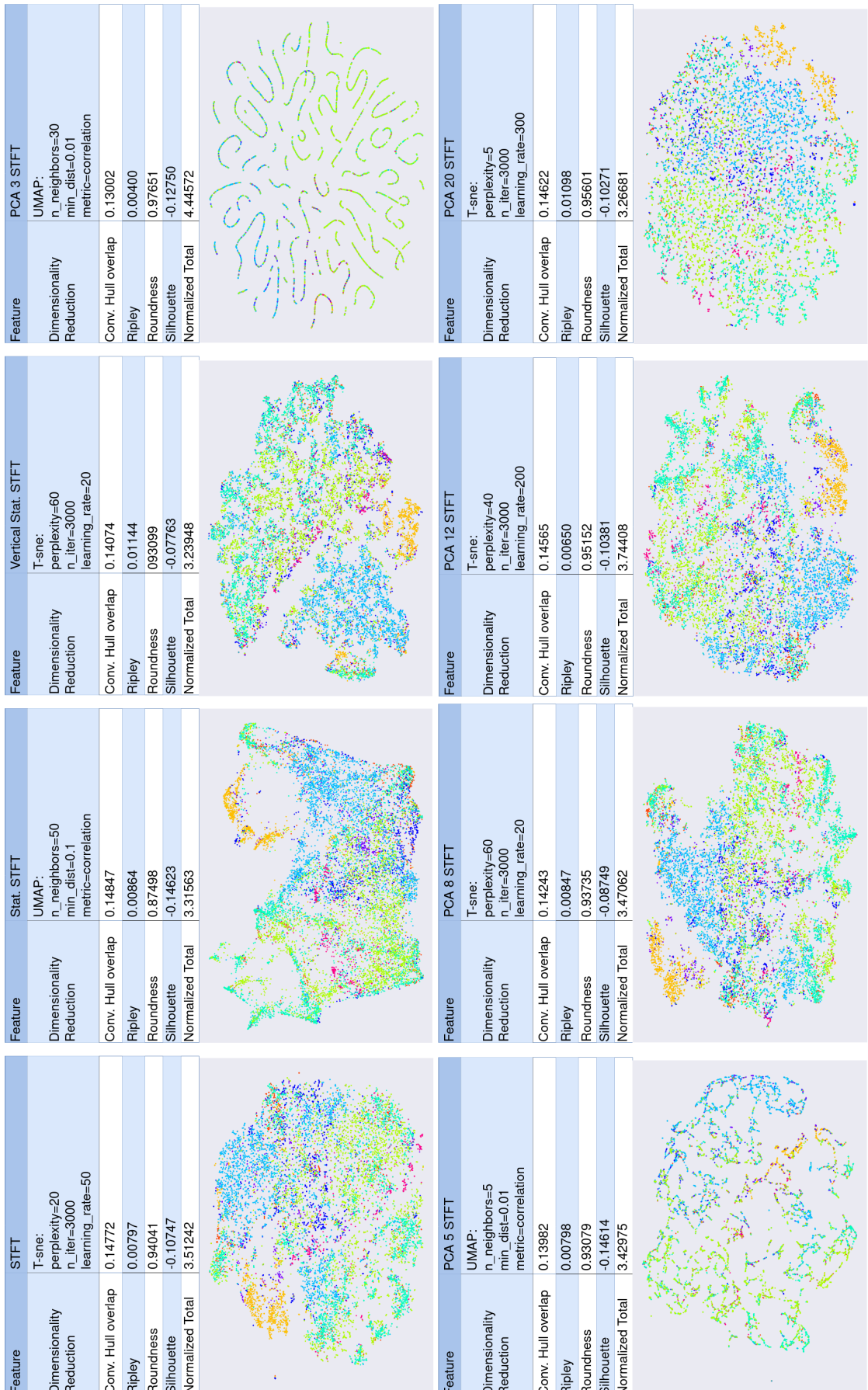


Figure 4.1: The best scoring plots for STFT features.

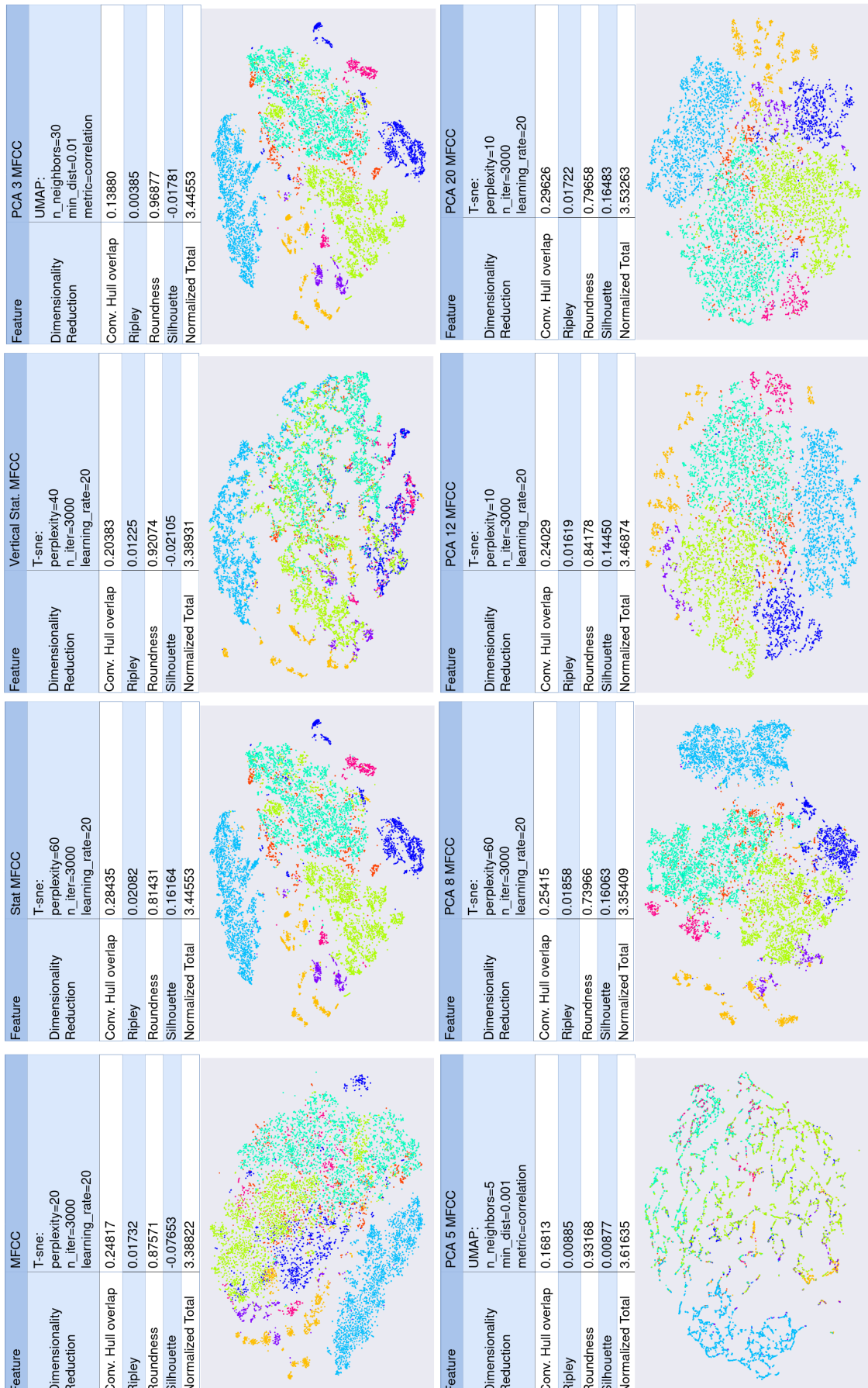


Figure 4.2: The best scoring plots for MFCC features.

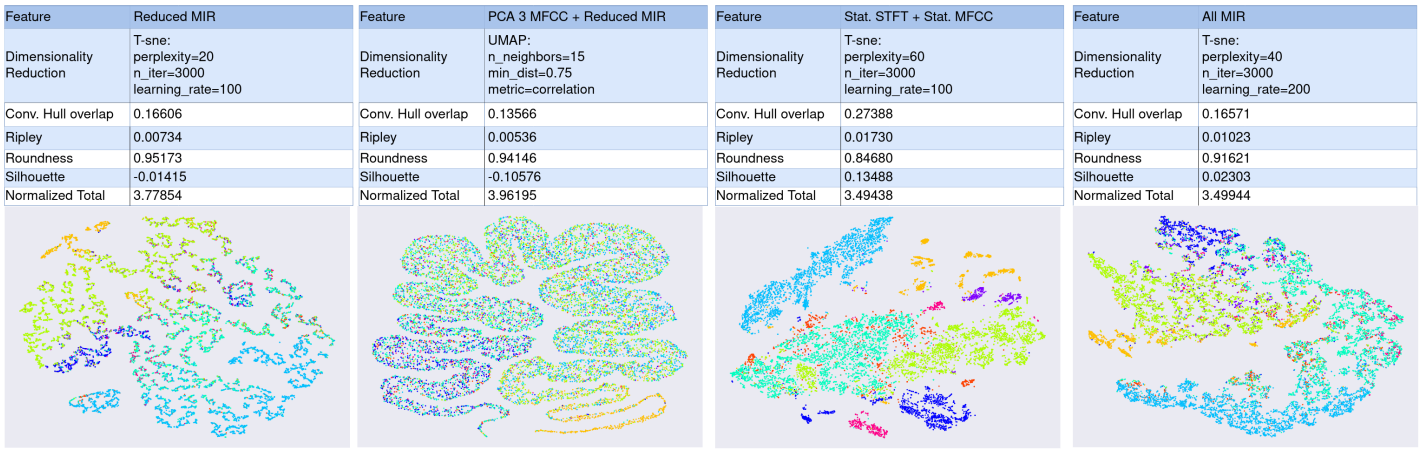


Figure 4.3: The best scoring plots for MIR features and combined feature sets.

4.2 The Ripley metric

Looking at the top scoring plots for the ripley metric presented in 4.7, it is clear that the PCA 3 plots do indeed score very highly in this regard. The first 8 top scoring ripley metrics come from a combination of PCA 3 + UMAP. My hypothesis is that each of the string like shapes is composed of points which are placed at distance apart from each other equal to that of the min dist UMAP parameter. 4.5 seems to show this as the points on the strings get slightly more farther apart as the *min dists* parameter increases. Also UMAP seems to have placed the strings themselves seem to be roughly equally spaced from each other. Thanks to this, if we take a circle from any point, we obtain an approximately equally distributed number of points. Hence, the high score of these plots for the Ripley metric. Since the points in the strings are tightly packed the Silhouette intra-cluster distance is low, the silhouette measure interprets as relatively well-clustered.

Let's see what the best plots are if we exclude the PCA 3 features. See 4.9. The plots are drastically different. A lot more inline with what might have been expected. It is interesting to see that the similar behaviour is present here also, although this time coming from a different feature, namely *reduced mir*. All these plots are also a result of UMAP.

4.3 The Silhouette Measure

But what happens if we remove the Ripley metric altogether? In ?? we can see the top 9 plots which scored highest without the Ripley metric. The difference is enormous. It is clear to see why this metric is so crucial for good-looking plots. These plots exhibit very clear and cleanly seperated clusters. These plots, however, would not be useful for the intended use case as the

clusters are *too* dense and would be hard to navigate. This is why the Ripley metric is indespensable.

4.4 Future work

Finding the correct metrics is crucial to correctly solving this problem. While it is probable that a combination of clustering and spatial measurements is the correct way to approach the problem, more work is still needed to find a set of metrics which would provide an optimal way of evaluating the plots in terms of both how well the timbral characteristics of the dataset are reflected

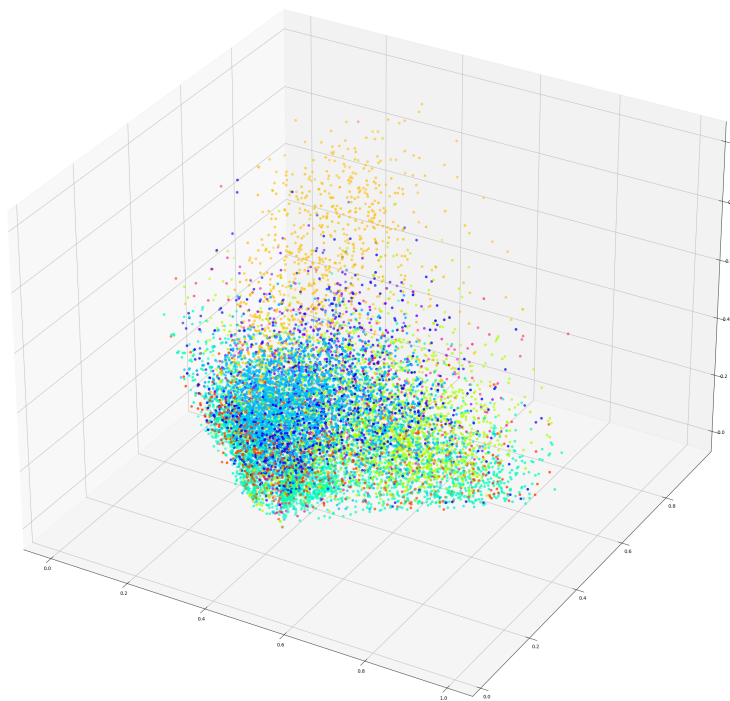


Figure 4.4: A plot of the PCA 3 MFCC feature

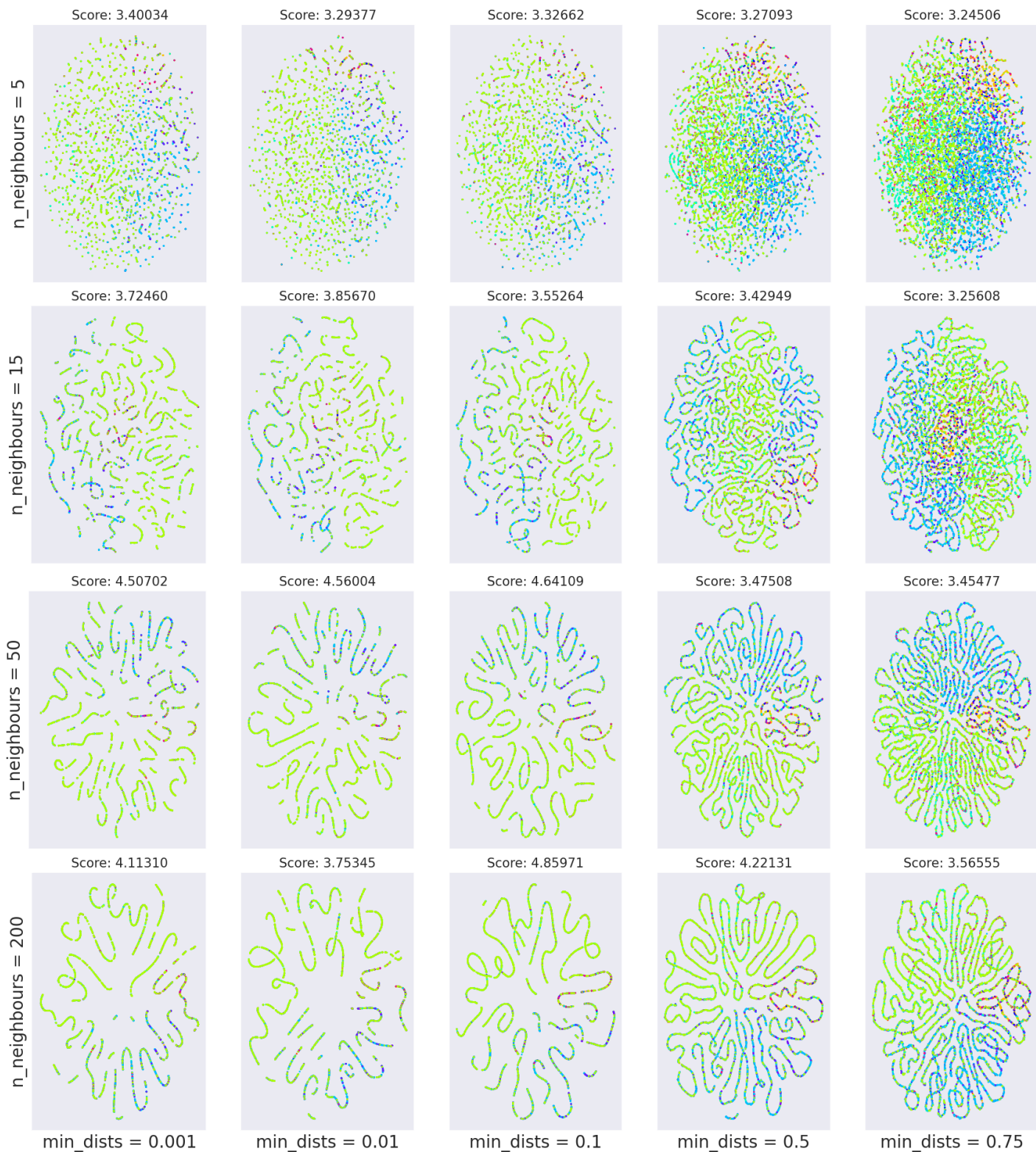


Figure 4.5: A grid search on the UMAP algorithm with the PCA 3 MFCC feature. As the value of n neighbours increases, the string-like pattern gets more pronounced.

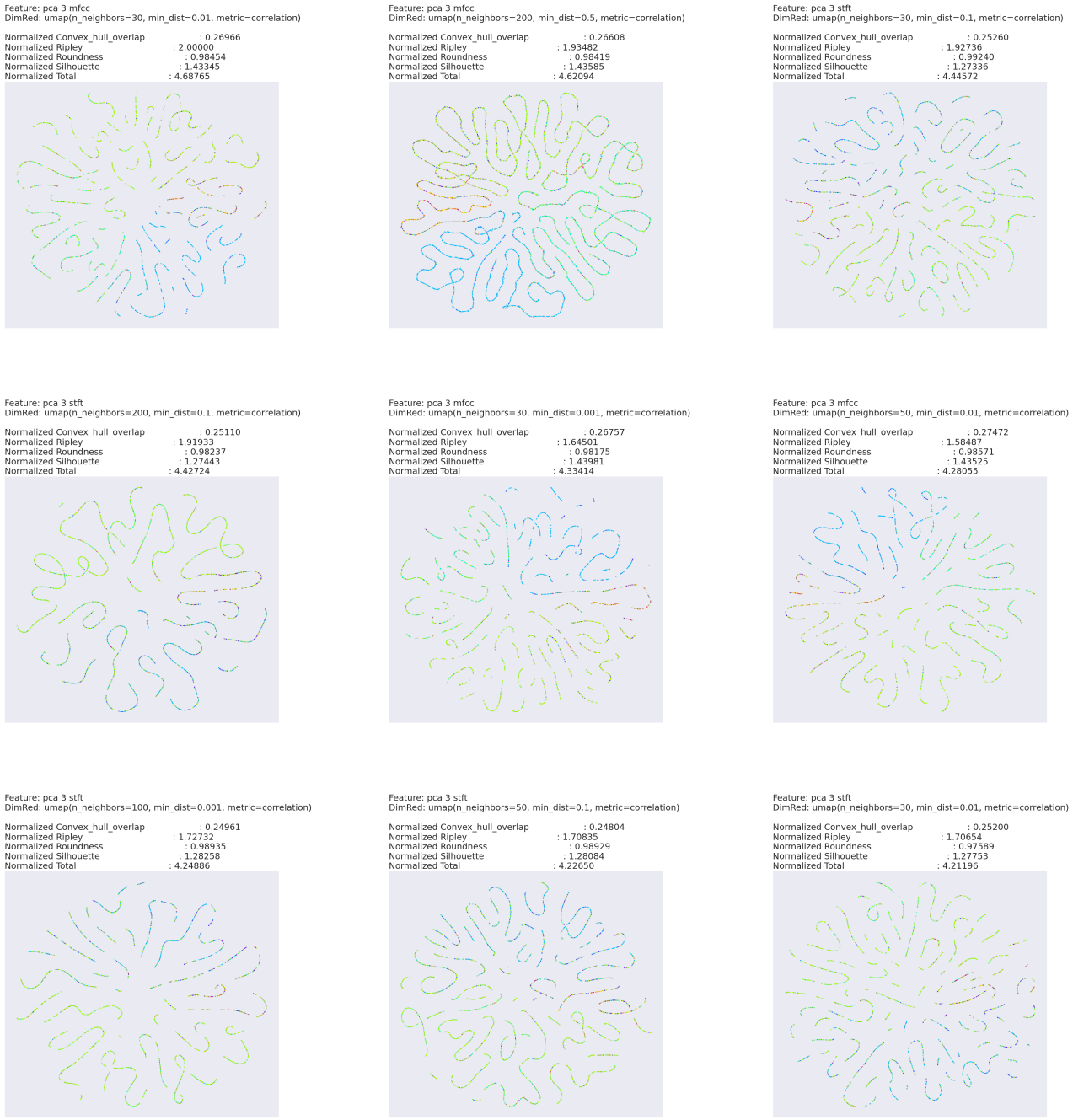


Figure 4.6: The top 9 scoring plots overall

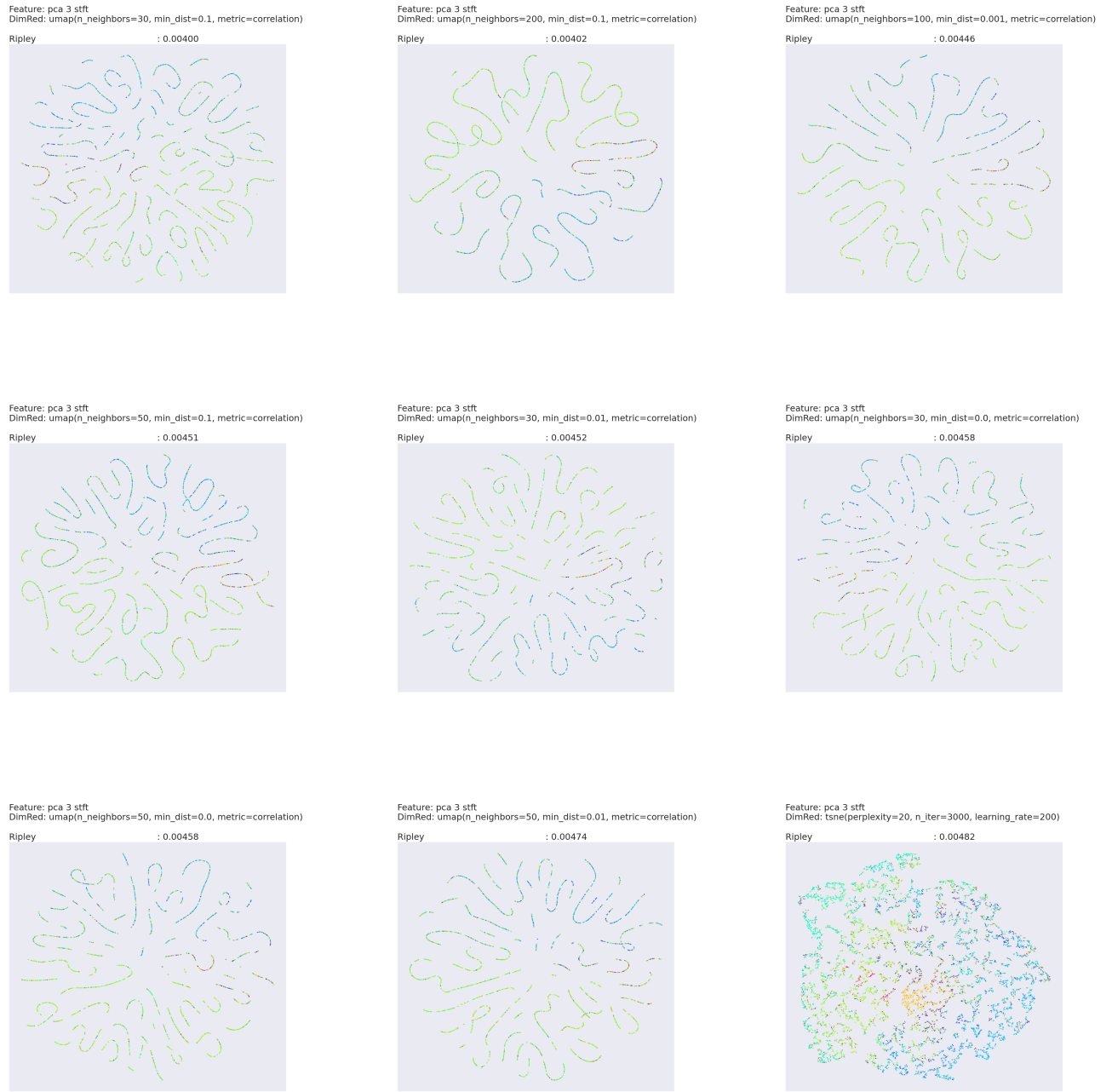


Figure 4.7: Top 9 scoring plots according to the Ripley metric

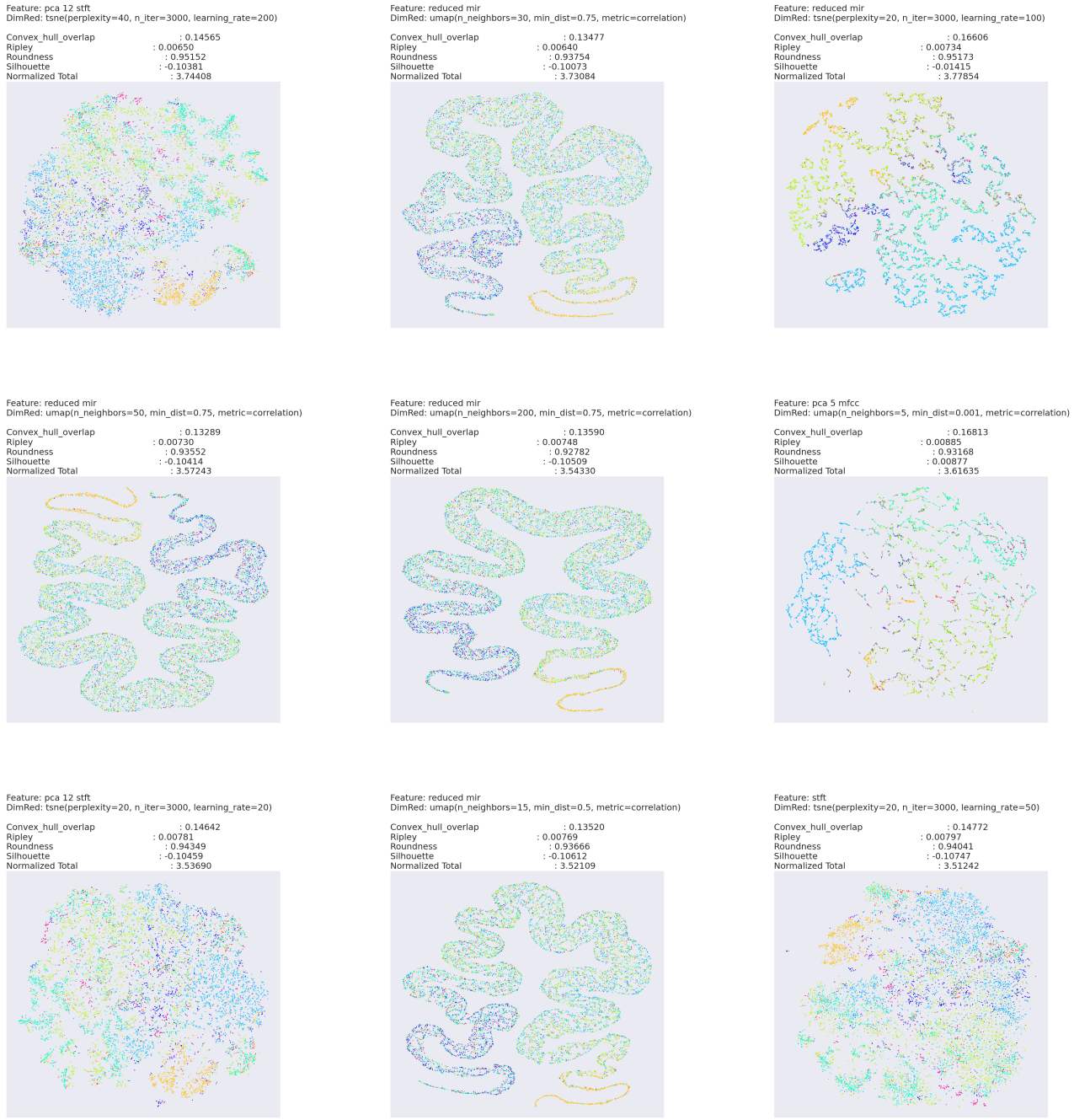


Figure 4.8: Top 9 scoring plots excluding the PCA 3 features

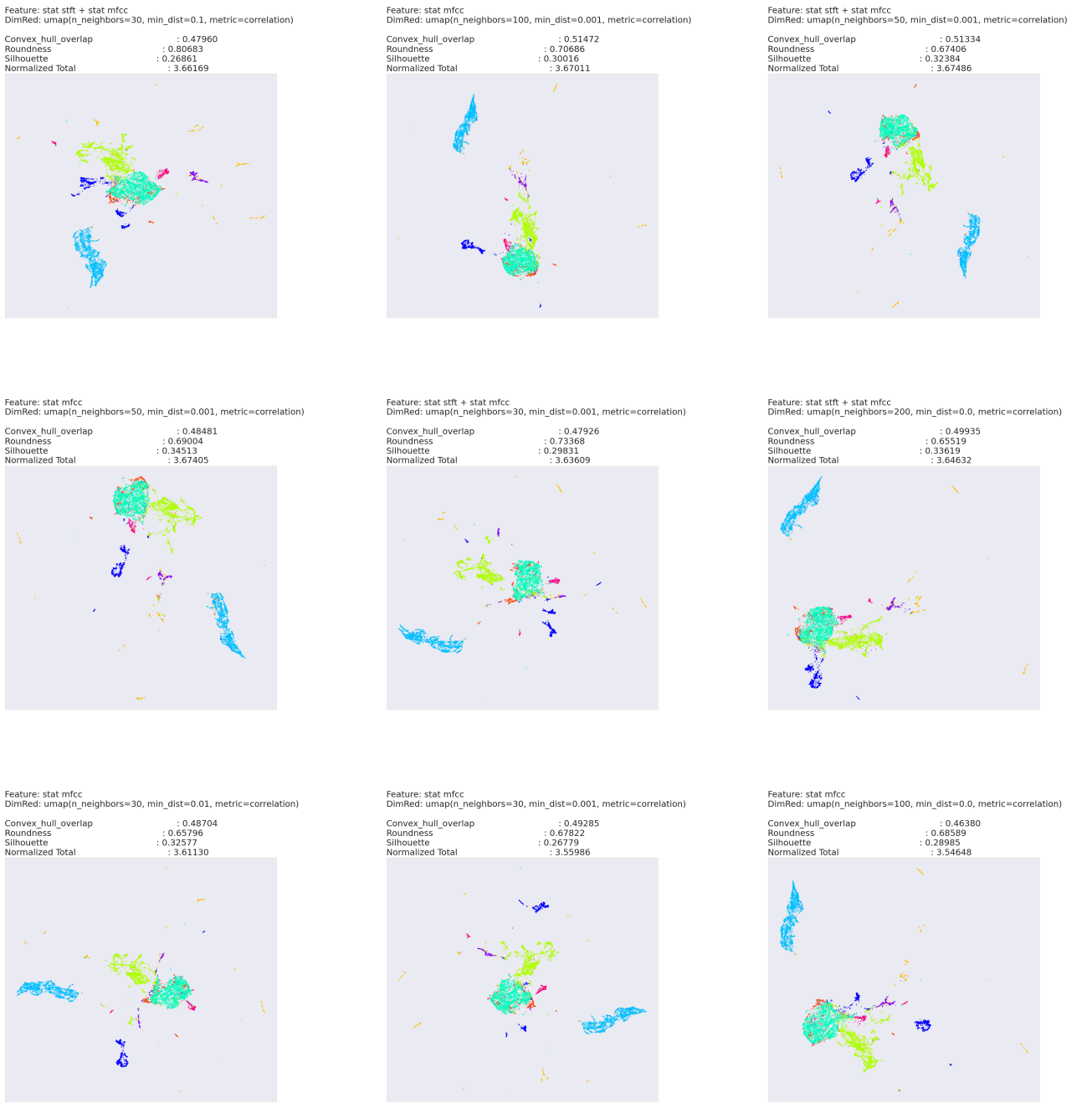


Figure 4.9: Top 9 scoring plots for metrics without the ripley measure

(i.e how well the sounds are clustered) and how comfortable the plot would be to use as a file browser (shape and density distribution).

In addition to this even more feature extraction methods such as wavenet autoencoders and methods from the field of MIR could be tested. There are also many more dimensionality reduction methods to experiment with.

4.5 Conclusion

The findings in this thesis were unexpected. Because of the findings of Hantrakul and Sarwate [16], I expected the combination of PCA + STFT + UMAP to do well. However the shape of the best-scoring plots were a big surprise and make the end results a lot more interesting than anticipated.

Bibliography

- [1] sklearn metrics silhouette score.
- [2] Rachel M Bittner, Magdalena Fuentes, David Rubinstein, Andreas Jansson, Keunwoo Choi, and Thor Kell. mirdata: Software for reproducible usage of datasets. In *International Society for Music Information Retrieval (ISMIR) Conference*, 2019.
- [3] S. Chakraborty, A. Roy, and G. Saha. Fusion of a complementary feature set with mfcc for improved closed set text-independent speaker identification. *2006 IEEE International Conference on Industrial Technology*, pages 387–390, 2006.
- [4] S. Davis and P. Mermelstein. Comparison of parametric representations for monosyllabic word recognition in continuously spoken sentences. *IEEE Transactions on Acoustics, Speech, and Signal Processing*, 28(4):357–366, 1980.
- [5] Jeremiah Deng, Christian Simmertacher, and Stephen Cranefield. A study on feature analysis for musical instrument classification. *IEEE transactions on systems, man, and cybernetics. Part B, Cybernetics : a publication of the IEEE Systems, Man, and Cybernetics Society*, 38:429–38, 05 2008.
- [6] Stephane Dupont, Thierry Ravet, Cecile Picard-Limpens, and Christian Frisson. Nonlinear dimensionality reduction approaches applied to music and textural sounds. *2013 IEEE International Conference on Multimedia and Expo (ICME)*, Jul 2013.
- [7] Leon Fedden. Comparative audio analysis with wavenet, mfccs, umap, t-sne and pca, 2017.
- [8] Geoffrey Hinton and Sam Roweis. Stochastic neighbor embedding. 15, 06 2003.

- [9] Yotam Mann Kyle McDonald, Manny Tan. The infinite drum machine. 2016.
- [10] Wentian Li, Jane E. Cerise, Yaning Yang, and Henry Han. Application of t-sne to human genetic data. *Journal of Bioinformatics and Computational Biology*, 15(04):1750017, 2017. PMID: 28718343.
- [11] Vincent Lostanlen, Carmine-Emanuele Cella, Rachel Bittner, and Slim Essid. Medley-solos-DB: a cross-collection dataset for musical instrument recognition. September 2019.
- [12] Brian McFee, Vincent Lostanlen, Alexandros Metsai, Matt McVicar, Stefan Balke, Carl Thomé, Colin Raffel, Frank Zalkow, Ayoub Malek, Dana, Kyungyun Lee, Oriol Nieto, Jack Mason, Dan Ellis, Eric Battenberg, Scott Seyfarth, Ryuichi Yamamoto, Keunwoo Choi, viktorandreevichmorozov, Josh Moore, Rachel Bittner, Shunsuke Hidaka, Ziyao Wei, nullmightybofo, Darío Hereñú, Fabian-Robert Stöter, Pius Friesch, Adam Weiss, Matt Vollrath, and Taewoon Kim. librosa/librosa: 0.8.0. July 2020.
- [13] L. Pols. Spectral analysis and identification of dutch vowels in monosyllabic words. 1977.
- [14] Popper Polsby, Daniel. The third criterion: Compactness as a procedural safeguard against partisan gerrymandering. *Yale Law & policy Review* 9.2 (1991): 301-353., 9:2579–2605, 2008.
- [15] Karthikeya Racharla, Vineet Kumar, Chaudhari Bhushan Jayant, Ankit Khairkar, and Paturu Harish. Predominant musical instrument classification based on spectral features. *2020 7th International Conference on Signal Processing and Integrated Networks (SPIN)*, Feb 2020.
- [16] Lamtharn (Hanoi) Hantrakul & Avneesh Sarwate. Klustr: A tool for dimensionality reduction and visualization of large audio datasets. <https://github.com/lamtharnhantrakul/klustr>, 2017.
- [17] Julius Smith. *Spectral Audio Signal Processing*. 01 2008.
- [18] L.J.P. van der Maaten and G.E. Hinton. Visualizing high-dimensional data using t-sne. *Journal of Machine Learning Research*, 9:2579–2605, 2008.

Appendices

Source Code

<https://github.com/luk-pio/audioviz>